



Published in final edited form as:

*J Am Chem Soc.* 2008 June 25; 130(25): 7856–7861. doi:10.1021/ja7109822.

## Crystal Structure of Thioflavin T Bound to the Peripheral Site of *Torpedo californica* Acetylcholinesterase Reveals How Thioflavin T Acts as a Sensitive Fluorescent Reporter of Ligand Binding to the Acylation Site

Michal Harel<sup>†</sup>, Leilani K. Sonoda<sup>‡</sup>, Israel Silman<sup>§</sup>, Joel L. Sussman<sup>†</sup>, and Terrone L. Rosenberry<sup>‡</sup>

Departments of Structural Biology and Neurobiology, Weizmann Institute of Science, Rehovot 76100, Israel, and Department of Neuroscience, Mayo Clinic College of Medicine, 4500 San Pablo Road, Jacksonville, Florida 32224

Terrone L. Rosenberry: rosenberry@mayo.edu

### Abstract

Acetylcholinesterase plays a key role in cholinergic synaptic transmission by hydrolyzing the neurotransmitter acetylcholine with one of the highest known catalytic rate constants. Hydrolysis occurs in a narrow and deep gorge that contains two sites of ligand binding: A peripheral site, or P-site, near the gorge entrance that contributes to catalytic efficiency both by transiently trapping substrate molecules as they enter the gorge and by allosterically accelerating the transfer of the substrate acyl group to a serine hydroxyl in an acylation site or A-site at the base of the gorge. Thioflavin T is a useful reporter of ligand interactions with the A-site. It binds specifically to the P-site with fluorescence that is enhanced ~1000-fold over that of unbound thioflavin T, and the enhanced fluorescence is quenched 1.5- to 4-fold when another ligand binds to the A-site in a ternary complex. To clarify the structural basis of this advantageous signal change, we here report the X-ray structure of the complex of thioflavin T with *Torpedo californica* acetylcholinesterase. The two aromatic rings in thioflavin T are coplanar and are packed snugly parallel to the aromatic side chains of Trp279, Tyr334, and Phe330. Overlays of this structure with the crystal structures of *Torpedo californica* acetylcholinesterase complexes with either edrophonium or *m*-(*N,N,N*-trimethylammonio)-2,2,2-trifluoroacetophenone, two small aromatic ligands that bind specifically to the A-site, indicate that the phenyl side chain of Phe330 must rotate to sterically accommodate both thioflavin T and the A-site ligand in the ternary complex. This rotation may allow some relaxation of the strict coplanarity of the aromatic rings in the bound thioflavin T and result in partial quenching of its fluorescence.

### Introduction

Acetylcholinesterase (AChE) terminates synaptic transmission at cholinergic synapses by rapid hydrolysis of the neurotransmitter acetylcholine (ACh).<sup>1</sup> It has become an important drug target because partial inhibition of AChE results in modest increases in ACh levels that can have therapeutic benefits; thus, AChE inhibitors that penetrate the blood-brain barrier

© 2008 American Chemical Society

Correspondence to: Terrone L. Rosenberry, rosenberry@mayo.edu.

<sup>†</sup>Department of Structural Biology, Weizmann Institute of Science.

<sup>‡</sup>Mayo Clinic College of Medicine.

<sup>§</sup>Department of Neurobiology, Weizmann Institute of Science.

have proved useful in the symptomatic treatment of Alzheimer's disease.<sup>2</sup> However, complete inactivation of AChE, which can occur with organophosphate and carbamate insecticides<sup>3</sup> and organophosphate chemical warfare agents,<sup>4</sup> leads to toxic accumulation of ACh and failure of cholinergic synaptic transmission, with consequent deterioration of neuromuscular junctions, flaccid muscle paralysis, and seizures in the central nervous system.

Kinetic and thermodynamic studies have revealed that inhibitors can interact with either or both of two binding sites in AChE,<sup>5,6</sup> and X-ray crystallography has provided information about the location of these sites.<sup>7-10</sup> A narrow gorge, ~20 Å deep, lined with aromatic residues, penetrates nearly to the center of the ~65 kDa catalytic subunits. Near the base of the gorge is the *acylation site* or A-site. This site includes a catalytic triad consisting of residue Ser200, His440 and Glu327. Similar triads are found in other hydrolases, and they promote acylation and deacylation of the serine residue by the substrate during catalytic turnover. An excellent model of the transition state for acylation by ACh was provided by *m*-(*N,N,N*-trimethylammonio)trifluoroacetophenone (TMTFA; see Figure 1 below).

The crystal structure of the complex of *Torpedo californica* AChE (*TcAChE*) with 4-oxo-*N,N,N*-trimethylpentanaminium (PDB code 2C5F) and with TMTFA (PDB code 1AMN) both indicate a tetrahedral adduct that nearly superimposes on a modeled structure of ACh in the A-site, and reveals that Trp84 in the A-site binds to the trimethylammonium group of ACh as acyl transfer to Ser200 is initiated.<sup>9</sup> Crystal structures also showed a binding site near the entrance of the active-site gorge that includes residues Trp279 and Asp72.<sup>9-11</sup> Ligands specific for this *peripheral site*, or P-site, include propidium<sup>6</sup> and the fasciculins - three very similar snake venom neurotoxins comprised of 61-amino acid polypeptides.<sup>12-14</sup> These P-site ligands are bulky and, to a large extent, lie outside the active-site gorge. Bis-quaternary, as well as long uncharged, ligands that span the 12-15 Å distance between the A- and P-sites,<sup>15-17</sup> can have high affinities and have been developed as therapeutic agents.<sup>18</sup>

One unique advantage of fluorescent ligands that bind selectively to the P-site is their ability to report on molecular interactions occurring at the A-site. The fluorescence of propidium is enhanced nearly 10-fold when it binds to the P-site, and this increase is sufficient to conduct titrations that quantify propidium affinity for the P-site and detect the formation of ternary complexes with propidium bound at the P-site and selective ligands like edrophonium (EDR) (Figure 1) bound at the A-site.<sup>6,19,20</sup> Thioflavin T (ThT) (Figure 1) is a fluorophore frequently used to detect amyloid structure in proteins,<sup>21</sup> but ligand-binding data indicate that it also binds with high selectivity to the P-site of AChE,<sup>22</sup> even though this site shows no indication of the  $\beta$ -structure typical of amyloid.

The fluorescence of ThT is increased ~1000-fold on binding to the P-site of human AChE; on further binding of an A-site ligand, such as EDR or TMTFA, to form a ternary complex, the fluorescence of the bound ThT is quenched 3-4-fold.<sup>22</sup> These features make ThT a more sensitive and versatile fluorescent reporter of ligand interactions with AChE than propidium. The quenching of fluorescence in the ternary complex occurs even though there is no spectral overlap, nor any obvious steric overlap (based on an absence of thermodynamic interaction), between the bound ligands.<sup>22</sup> This change in fluorescence is perhaps the most direct evidence for conformational interaction between the P- and A-sites that has been obtained. Certain substrates, including acetylthiocholine (ATCh), appear to take functional advantage of this conformational interaction. These substrates can bind to both the P- and the A-sites, as initially indicated by a competition between ATCh and fasciculin for binding to the P-site,<sup>23</sup> and confirmed clearly in X-ray structures of several AChE complexes, including those with ACh, choline, ATCh, thiocholine and the nonhydrolysable ACh

analogue, 4-oxo-*N,N,N*-trimethylpentanaminium.<sup>24,25</sup> Acylation at the A-site is accelerated when a second substrate molecule is bound at the P-site. Strong evidence supporting this model of substrate activation was obtained from titrations with ThT. These titrations provided thermodynamic estimates of substrate affinities for the A- and P-sites that were in complete agreement with kinetic estimates of these affinities derived from the substrate activation model.<sup>26</sup>

In view of the sensitivity of ThT fluorescence to the conformation of residues that contact ThT, it is important to obtain three-dimensional structures of binary and ternary complexes of ThT with AChE. Such structures may provide insight into the molecular details of conformational interaction between the P- and A-sites.

## Materials and Methods

### Materials

Thioflavin T chloride (Sigma) was recrystallized as described.<sup>22</sup> *TcAChE* was purified from the electric organ tissue of *T. californica*,<sup>11,27</sup> and active site concentrations were determined by fluorogenic titration with *N*-methyl-(7-dimethylcarbamoyl)quinolinium iodide.<sup>28</sup> Recombinant domain IV of mouse laminin  $\beta 2$ , expressed in 293 cells,<sup>29</sup> was a gift from Dr. Takako Sasaki (The Shriners Hospital for Children, Portland, OR).

### Crystallographic Analysis

Trigonal *P3<sub>2</sub>21**TcAChE* crystals, in which the active-site gorge is solvent-accessible, were grown by the batch-under-oil method,<sup>30</sup> using a Douglas Instruments IMPAX 1–5 robot. In order to obtain the *P3<sub>2</sub>21* *TcAChE* crystals, the protein solution used was a 1:4 (v/v) mixture of *TcAChE* (13.7 mg/ml) and domain IV of mouse laminin  $\beta 2$  (4.7 mg/ml).<sup>29</sup> *TcAChE* was found to crystallize from this mixture in spacegroup *P3<sub>2</sub>21*. The batch drops contained 0.25  $\mu$ L of the protein mixture, 0.25  $\mu$ L of Hampton Research Index #85 solution (25% PEG 3350, 0.2 M MgCl<sub>2</sub>, 0.1 M Tris, pH8.5) and 0.1  $\mu$ L of 1 M MgCl<sub>2</sub>. Crystals grew to 0.2  $\times$  0.2  $\times$  0.2 mm within 1 week at 18 °C. A supersaturated aqueous solution of ThT in 60% Index #85 was diluted 1:10, and a 0.1  $\mu$ L aliquot was added to a drop containing the crystals (final ThT concentration of 250  $\mu$ M). X-ray data were collected 5 days after the addition of ThT.

X-ray data to 2.8 Å resolution were collected under cryogenic conditions, “in-house” at the Weizmann Institute of Science, on a Rigaku R-AXIS IV++ image plate area detector. Data collection and refinement statistics are shown in Table 1.

The data were reduced with the XDS program,<sup>31</sup> refined with CNS,<sup>32</sup> and graphically fitted using COOT.<sup>33</sup> Coordinates and structure factors were deposited in the PDB with entry code 2J3Q.

### Fluorescence Determinations of the Binding of Thioflavin T to *TcAChE*

ThT fluorescence was measured with excitation at 450 nm and emission at 490 nm (slits 10 and 20 nm, respectively), in 60 mM NaCl, 40 mM sodium phosphate buffer (pH 7.0) and 0.04% Triton X-100, on a Perkin-Elmer LS-50B luminescence spectrometer thermostatted at 25 °C. Samples were introduced into a Hi-Tech SFA 20 stopped-flow apparatus by mixing equal volumes (300  $\mu$ l) of AChE and combined inhibitors, and the continuous fluorescence signal (F) was recorded for 3–4 min. Average F values were corrected for inner filter effects<sup>34</sup> as described previously.<sup>26</sup> Data were analyzed in accordance with Scheme 1, which assumes that AChE (*E*) can form the indicated binary and ternary complexes with ThT (*L*) and EDR (*I*). Ligand bound at the P-site in Scheme 1 is designated by the subscript P, while ligand bound at the A-site has no subscript. Rate equations corresponding to an equilibrium

formulation of Scheme 1 were solved in the numerical integration program SCoP (Simulation Resources, Inc., Redlands, CA; version 3.52), and values of  $F$  were fitted in a two-step process.<sup>22</sup> Initial fitting was conducted in the absence of EDR, with the known total concentrations  $E_{\text{tot}}$  and  $L_{\text{tot}}$  and the known fluorescence intensity coefficient for free ThT ( $f_L$ ) inserted as fixed input parameters, and  $K_{Lp}$  and the intensity coefficient for thioflavin bound to the P-site ( $f_{ELp}$ ) as the calculated output parameters. This analysis revealed small amounts of an apparent ternary complex involving ThT bound to both the P- and A-sites, so the fitting was extended to obtain  $K_{LpL}$  and the intensity coefficient  $f_{ELpL}$  as additional output parameters. The fitting in principle also depended on  $K_L$  and the intensity coefficient  $f_{EL}$ , but over a reasonable range of values ( $K_L/K_{LpL} > 0.25$  and  $f_{EL}/f_{ELp} < 0.2$ ) the values of these parameters were unimportant (<30% change in the output parameters). Greater uncertainty arose because  $K_{LpL}$  and  $f_{ELpL}$  were highly correlated, preventing unique assignments. Consequently, in the second fitting step in the presence of EDR, a reasonable range of  $f_{ELpL}$  ( $f_{ELpL}/f_L = 100\text{--}400$ ) and the corresponding fitted value of  $K_{LpL}$  ( $34\text{--}5\ \mu\text{M}$ ) were examined as fixed input parameters along with  $E_{\text{tot}}$ ,  $L_{\text{tot}}$ ,  $I_{\text{tot}}$  and  $f_L$ , and  $K_{Lp}$ ,  $K_I$ ,  $K_{LpI}$ ,  $f_{ELp}$ ,  $f_{ELpI}$  were obtained as fitted outputs.

## Results

### Fluorescence of ThT is Strongly Enhanced in Binary Complexes with *TcAChE* and Partially Quenched when an A-Site Ligand is Added to Form a Ternary Complex

We show in this report that a key residue involved in the binding of ThT to *TcAChE* is Phe330. Since the corresponding residue in human AChE (hAChE) is a tyrosine (Tyr337), it was important to confirm that ThT complexes involving *TcAChE* show fluorescence features similar to those involving hAChE. Titration of *TcAChE* with ThT (Figure 2A) gave the same 1200-fold increase in the relative fluorescence intensity of the bound ligand ( $f_{ELp}/f_L$ ) previously observed with hAChE.<sup>22</sup> However, at high concentrations of ThT, a decrease in fluorescence occurred that had not been seen with hAChE. We interpreted this decrease to reflect the low-affinity binding of a second molecule of ThT to the A-site of *TcAChE* (see Scheme 1). As noted in the Introduction, the binding of a ligand to the A-site in the ThT/hAChE complex would be expected to result in partial quenching of the fluorescence of thioflavin T bound at the P-site. The affinity of ThT for the A-site of *TcAChE* was at least an order of magnitude lower than that for the P-site, and incorporation of this A-site binding did not obscure further thermodynamic analysis with the A-site ligand EDR, but did lower the precision with which some binding parameters could be determined (see Experimental Procedures).

We next examined the effect of increasing EDR concentrations on the fluorescence of bound ThT, and observed a decrease in fluorescence as EDR saturated the A-site (Figure 2B). Fitting of the data to Scheme 1 gave values of  $K_{Lp}$  for ThT and  $K_I$  for EDR, and indicated a slight decrease in the affinities of the ligands in the ternary complex relative to the binary complex ( $K_{LpI}/K_I = 4 \pm 1$ ). Almost no decrease in these relative affinities had been observed with hAChE ( $K_{LpI}/K_I = 1.12 \pm 0.02$ <sup>22</sup>). However, the binding of EDR decreased the fluorescence of ThT in the ternary complex ( $f_{ELp}/f_{ELpI}$ ) by a factor of  $3.4 \pm 0.6$ , comparable to the decrease previously seen with hAChE ( $2.76 \pm 0.02$ ). These data thus confirm that the fluorescence features of ThT complexes involving *TcAChE* are essentially the same as those involving hAChE.

### X-Ray Structure of the ThT/*TcAChE* Complex

We earlier obtained structures of a number of complexes of *TcAChE* with A-site ligands,<sup>15,35</sup> and with ligands spanning the A- and P-sites,<sup>16,36</sup> by diffusing the ligands into the protein crystals in the  $P3_121$  trigonal crystal form. In this crystal form, the P-site at the

entrance to the active-site gorge is blocked by a segment of a symmetry-related *TcAChE* molecule. Hence, it was not possible to obtain structures of complexes with bulky P-site ligands using this approach with such crystals. A breakthrough was achieved when it was discovered that crystals of *TcAChE* could be grown in the presence of gallamine triethiodide, a P-site ligand with relatively low affinity, to yield a  $P3_221$  trigonal crystal form in which the entrance to the active-site gorge is more open.<sup>37</sup> Since then, several other crystallization additives have been found to yield crystal forms of *TcAChE* in which the P-site is accessible to bulky ligands.<sup>38,39</sup> In the present study, mouse recombinant domain IV of laminin  $\beta 2^{29}$  was used as a crystallization additive to obtain the  $P3_221$  crystals. The rms deviation of the C $\alpha$  chain between the  $P3_221$  and the  $P3_121$  crystal structures is only 0.3 Å, indicating a virtually identical overall conformation of the two molecules. However, P-site ligands could be soaked into the  $P3_221$  crystal form;<sup>37</sup> indeed, a crystal structure at 2.8 Å resolution was obtained upon soaking such *TcAChE* crystals with ThT (Figure 3).

The X-ray structure of the ThT/*TcAChE* complex refined to an R factor of 19.6% and an R-free of 25.1%. Residues 4–536 of *TcAChE* were traced in the electron density map, as well as one molecule of ThT, 121 water molecules, and 3 *N*-acetylglucosamine moieties attached to Asn residues 59, 416 and 457. Two bound Mg<sup>2+</sup> ions, derived from the mother liquor, are seen in the electron density map. One of these Mg<sup>2+</sup> ions is in contact with Glu268O $\epsilon$ 1 and O $\epsilon$ 2 and with His264N $\epsilon$ 2 (2.22, 3.34, and 2.66 Å, respectively); the second with Asp392O $\delta$ 2, Asp326O $\delta$ 1 and a water molecule (2.35, 2.43, and 2.36 Å, respectively). The positions of the two Mg<sup>2+</sup> ions superimpose, respectively, on those of a Mg<sup>2+</sup> ion and a Zn<sup>2+</sup> ion in a structure of *TcAChE* crystallized in the presence of MgCl<sub>2</sub> (Anne Nicolas, unpublished results).

Figure 3 shows that the planar ThT molecule is lodged in the upper part of the active-site gorge, within the P site, making nonbonding interactions with four of the aromatic side-chains that line the gorge surface, viz. Tyr70, Tyr121, Trp279 and Phe330. Superposition of the ThT/*TcAChE* structure on that of native *TcAChE* (PDB code 1EA5) yields rms = 0.33 Å (for 532 C $\alpha$  atoms), and shows that all the gorge side-chains maintain their native conformation in the complex and that the ThT molecule fills the space within the gorge previously occupied by four water molecules.

More detailed inspection reveals that the benzothiazole ring of ThT is stacked against Trp279, and that its dimethylaminophenyl moiety is nearly coplanar with the phenyl group of Phe330 at a distance of 3.5 Å (Figure 3). Other interactions between ThT and the protein include a 3.2 Å contact from Tyr121OH to the dimethylaminophenyl moiety and 3.4 and 3.7 Å contacts from Tyr70 and Tyr334 to the benzothiazole ring, respectively.

### Overlay of the ThT/*TcAChE* Structure with the Crystal Structures of A-Site Complexes

Since, as mentioned in the Introduction, the A-site ligands, EDR and TMTFA, quench the fluorescence of the ThT/*TcAChE* complex,<sup>22</sup> we overlaid both EDR from the EDR/*TcAChE* complex<sup>15</sup> (Figure 4A) and TMTFA from the TMTFA/*TcAChE*<sup>9</sup> complex<sup>9</sup> (not shown) on the ThT/*TcAChE* crystal structure. From these overlays it is apparent that the ThT/*TcAChE* structure can sterically accommodate both EDR and TMTFA at the A-site; the aromatic rings of both EDR and TMTFA, in their respective complexes, are nearly coplanar with Trp279/ThT/Phe330 in the ThT/*TcAChE* complex. However, if one does the reverse, and overlays ThT from the ThT/*TcAChE* structure on the crystal structures of either EDR/*TcAChE* (Figure 4B) or TMTFA/*TcAChE* (not shown), it can be seen that there is a clash of the dimethylaminophenyl moiety of the ThT molecule with the phenyl side-chain of Phe330. The reason for this clash is that in both the EDR/*TcAChE* and TMTFA/*TcAChE* structures the phenyl ring is rotated  $\sim 115^\circ$  relative to its orientation in both the native *TcAChE* and ThT/*TcAChE* structures.



## Discussion

Crystal structures of *TcAChE* complexes with A-site ligands,<sup>11,15,40</sup> with the P-site ligands fasciculin<sup>9,11</sup> and propidium,<sup>10</sup> and with ligands which span the two sites,<sup>15,36,37</sup> show remarkably few differences in conformation of the entire active-site gorge relative to native *TcAChE*. These observations indicate that the binding of these ligands does not induce large (and potentially slow) conformational changes in the active site, as might be expected for an enzyme like AChE that is built for unusually high catalytic speed. The structure of the ThT/*TcAChE* complex also shows few changes from that of native *TcAChE*, and the basis of the enhanced ThT fluorescence in this complex and its partial quenching in ternary complexes are of interest. The fluorescence of ThT has been shown to depend on solvent viscosity,<sup>41</sup> with a relationship previously described for a class of fluorescent dyes called molecular rotors.<sup>42,43</sup> These dyes show increased fluorescence when introduced into high-viscosity media due to a decreased torsional relaxation. The X-ray structure of the ThT/*TcAChE* complex presented here shows the ThT rings system in a coplanar position packing snugly parallel to Trp279, Tyr334 and Phe330. This packing causes a decrease in torsional relaxation and, hence, the increase in fluorescence.

The structures of complexes of *TcAChE* with bis-quaternary<sup>15,36</sup> and other gorge-spanning ligands<sup>16,37-39,44,45</sup> confirm that they bridge the A- and P-sites and traverse the region occupied by the bound ThT. In some of these structures the bifunctional ligands display contacts with Trp279 and Phe330 of *TcAChE* that bear some similarity to those made by ThT. Thus, in the BW284C51/*TcAChE* complex<sup>36</sup> (Figure 1) (PDB code 1E3Q), one quaternary phenylammonium group of the symmetric bifunctional ligand interacts with Trp279, with the two aromatic rings being coplanar, and an allyl group at its other extremity makes a strong hydrophobic interaction with Phe330. The anti-Alzheimer disease drug donepezil (E2020 or Aricept) also spans the A- and P-sites. Its indanone ring stacks against the indole ring of Trp279, and the charged nitrogen of a piperidine ring, separated by one methylene group from the indanone ring, makes a cation- $\pi$  interaction with the phenyl ring of Phe330.<sup>16</sup> In the crystal structure of the complex of *TcAChE* with the anticancer prodrug CPT-11 (PDB code 1U65), another ligand that spans the A- and P-sites,<sup>37</sup> the planar camptothecin moiety superimposes on the planar benzothiazole ring of ThT and stacks against Trp279. The terminal piperidine moiety of CPT-11 occupies the same space as the quaternary ammonium moiety of EDR at the A-site, and the penultimate piperidino ring stacks against the phenyl ring of Phe330. However, in all three of these complexes this phenyl ring rotates away from its position in the ThT/*TcAChE* complex to allow the ligand to span the A- and P-sites.

The packing of ThT with its rings snugly parallel to Trp279, Tyr334, and Phe330 reveals a precise ligand location that has not been previously observed in X-ray structures of AChEs complexed with other ligands specific for the P-site. In the complex of mouse AChE (mAChE) with the P-site ligand gallamine (Figure 1) (PDB code 1N5M), the aromatic moiety of the ligand, which is the only part of the gallamine molecule seen in the structure, is positioned similarly to ThT, making stacking contacts with both Trp286 and Tyr341 but not Tyr337 (Trp 279, Tyr334, and Phe 330, respectively, in *TcAChE*).<sup>10</sup> In structures of mAChE complexes with two other ligands that bind selectively to the P-site, propidium and decidium, the ligands interacted with Trp286 but were reported to extend outward along the enzyme surface.<sup>10</sup> The location and orientation of ThT within the P-site may help to explain why this fluorophore is such a useful reporter for ligand binding at the A-site. The side chain of Phe330 in the ThT/*TcAChE* complex has the same conformation as in the native 1.8 Å *TcAChE* X-ray structure (PDB code 1EA5), and is coplanar with the dimethylaminophenyl moiety of ThT. In X-ray structures of the complexes of *TcAChE* with both EDR and TMTFA, two small quaternary aromatic ligands that bind specifically to the A-site, the  $\chi_1$

angle of Phe330 is rotated  $\sim 115^\circ$  from its position in native *TcAChE*.<sup>9,15</sup> This rotation is very similar to that observed upon binding of the substrate, acetylthiocholine, or of the product, thiocholine.<sup>24,25</sup> As shown in Figure 4B, this rotation produces a clash between Phe330 and the proximal ring of ThT, if the latter occupies the same position as it occupies in the ThT/*TcAChE*. Hence, the phenyl ring of Phe330 cannot be assumed to occupy the same position in a putative EDR/ThT/*TcAChE* ternary complex as in the ThT/*TcAChE*, and must rotate. This rotation may allow some relaxation of the strict coplanarity of the aromatic rings of the bound ThT and of the enzyme, thus resulting in partial quenching of its fluorescence. Indeed, attempts to obtain crystals of such a ternary complex, as well as of the analogous ternary complex with TMTFA, have been unsuccessful, since crystals of both the EDR/*TcAChE* and TMTFA/*TcAChE* complexes lost their diffracting power after ThT had been soaked into them. This implies that, in both cases, formation of the ternary complex produced a conformational change that damaged the crystal lattice. Similarly, it was earlier reported that soaking trigonal crystals (spacegroup  $P3_121$ ) of native *TcAChE* with a galanthamine derivative that could not be accommodated by the native conformation of the active-site gorge resulted in loss of diffracting power of these otherwise robust crystals.<sup>38</sup> Formation of an EDR/ThT/*TcAChE* or a TMTFA/ThT/*TcAChE* ternary complex results in a 3–4-fold quenching of bound ThT fluorescence. Another small A-site ligand, 3-(acetamido)-*N,N,N*-trimethylanilinium, for which a crystal structure in complex with AChE is lacking, also produces strong (viz. 3–4-fold) quenching of ThT fluorescence in the ternary complex,<sup>26</sup> while the A-site ligand carbachol quenches ThT fluorescence by only 35%. (T.L. Rosenberry, unpublished data). Carbachol (Figure 1), an ACh analog, probably produces a change in conformation of Phe330 similar to that seen in the crystal structures of the complexes with ATCh and thiocholine,<sup>24</sup> which in turn, is similar to those produced by EDR and TMTFA. The smaller quenching produced by carbachol, compared to the much larger quenching produced by EDR and TMTFA, may be due to the fact that it does not participate in a comparable stacking array involving stacking of the ThT with the *TcAChE* aromatic rings or that it imposes a smaller rotation of the phenyl ring of Phe330 from coplanarity with the dimethylaminophenyl moiety of ThT in the ternary complex.

## Acknowledgments

This study was supported by grants from The Israel Science Foundation (to JLS and IS), from the Israel Ministry of Science, Culture, and Sport to the Israel Structural Proteomics Center (ISPC), the European Commission Sixth Framework Research and Technological Development Programme (Grant No.: 031220), the National Institutes of Health (Grant NS-16577 to TLR), the Muscular Dystrophy Association of America (to TLR), the Benziyo Center for Neuroscience (to IS), the Nalvyco Foundation and the Divadol Foundation. We thank Dr. Takako Sasaki for the sample of domain IV of laminin  $\beta_2$ , and Michal Cohen and Lilly Toker for the *TcAChE* preparations used. J.L.S. is the Morton and Gladys Pickman Professor of Structural Biology.

## References

1. Silman I, Sussman JL. *Curr Opin Pharmacol*. 2005; 5:293–302. [PubMed: 15907917]
2. Giacobini, E. Cholinesterase inhibitors: from the Calabar bean to Alzheimer therapy In *Cholinesterases and Cholinesterase Inhibitors*. Giacobini, E., editor. Martin Dunitz; London: 2000. p. 181-226.
3. Casida JE, Quistad GB. *Annu Rev Entomol*. 1998; 43:1–16. [PubMed: 9444749]
4. Millard CB, Broomfield CA. *J Neurochem*. 1995; 64:1909–1918. [PubMed: 7722478]
5. Changeux JP. *Mol Pharmacol*. 1966; 2:369–392. [PubMed: 5970686]
6. Taylor P, Lappi S. *Biochemistry*. 1975; 14:1989–1997. [PubMed: 1125207]
7. Sussman JL, Harel M, Frolow F, Oefner C, Goldman A, Toker L, Silman I. *Science*. 1991; 253:872–879. [PubMed: 1678899]
8. Bourne Y, Taylor P, Marchot P. *Cell*. 1995; 83:503–512. [PubMed: 8521480]
9. Harel M, Quinn DM, Nair HK, Silman I, Sussman JL. *J Am Chem Soc*. 1996; 118:2340–2346.

10. Bourne Y, Taylor P, Radic Z, Marchot P. *EMBO J.* 2003; 22:1–12. [PubMed: 12505979]
11. Raves ML, Harel M, Pang YP, Silman I, Kozikowski AP, Sussman JL. *Nat Struct Biol.* 1997; 4:57–63. [PubMed: 8989325]
12. Karlsson E, Mbugua PM, Rodriguez-Ithurralde D. *J Physiol (Paris).* 1984; 79:232–240. [PubMed: 6530667]
13. Marchot P, Khelif A, Ji YH, Masnuelle P, Bourgis PE. *J Biol Chem.* 1993; 268:12458–12467. [PubMed: 8509385]
14. Harel M, Kleywegt GJ, Ravelli RBG, Silman I, Sussman JL. *Structure.* 1995; 3:1355–1366. [PubMed: 8747462]
15. Harel M, Schalk I, Ehret-Sabatier L, Bouet F, Goeldner M, Hirth C, Axelsen PH, Silman I, Sussman JL. *Proc Natl Acad Sci USA.* 1993; 90:9031–9035. [PubMed: 8415649]
16. Kryger G, Sillman I, Sussman JL. *Structure.* 1999; 7:297–307. [PubMed: 10368299]
17. Bourne Y, Kolb HC, Radic Z, Sharpless KB, Taylor P, Marchot P. *Proc Natl Acad Sci USA.* 2004; 101:1449–1454. [PubMed: 14757816]
18. Du DM, Carlier PR. *Curr Pharm Des.* 2004; 10:3141–3156. [PubMed: 15544504]
19. Berman HA, Decker MM, Nowak MW, Leonard KJ, McCauley M, Baker WM, Taylor P. *Mol Pharmacol.* 1987; 31:610–616. [PubMed: 3600605]
20. Barak D, Ordentlich A, Bromberg A, Kronman C, Marcus D, Lazar A, Ariel N, Velan B, Shafferman A. *Biochemistry.* 1995; 34:15444–15452. [PubMed: 7492545]
21. LeVine, H, III. Quantification of  $\beta$ -sheet amyloid fibril structures with thioflavin T. In: Wetzel, R., editor. *Methods in Enzymology.* Vol. 309. Academic Press; Orlando, FL: 1999. p. 274-284.
22. De Ferrari GV, Mallender WD, Inestrosa NC, Rosenberry TL. *J Biol Chem.* 2001; 276(2):23282–23287. [PubMed: 11313335]
23. Szegletes T, Mallender WD, Rosenberry TL. *Biochemistry.* 1998; 37:4206–4216. [PubMed: 9521743]
24. Colletier JP, Fournier D, Greenblatt HM, Stojan J, Sussman JL, Zaccai G, Silman I, Weik M. *EMBO J.* 2006; 25:2746–2756. [PubMed: 16763558]
25. Bourne Y, Radic Z, Sulzenbacher G, Kim E, Taylor P, Marchot P. *J Biol Chem.* 2006; 281:29256–29267. [PubMed: 16837465]
26. Johnson JL, Cusack B, Davies MP, Fauq A, Rosenberry TL. *Biochemistry.* 2003; 42:5438–5452. [PubMed: 12731886]
27. Sussman JL, Harel M, Frolow F, Varon L, Toker L, Futerman AH, Silman I. *J Mol Biol.* 1988; 203:821–823. [PubMed: 2850366]
28. Rosenberry TL, Bernhard SA. *Biochemistry.* 1971; 10:4114–4120. [PubMed: 5168614]
29. Sasaki T, Mann K, Miner JH, Miosge N, Timpl R. *Eur J Biochem.* 2002; 269:431–442. [PubMed: 11856301]
30. D'Arcy A, MacSweeney A, Stihle M, Haber A. *Acta Crystallogr D Biol Crystallogr.* 2003; 59:396–399. [PubMed: 12554964]
31. Kabsch W. *J Appl Crystallogr.* 1993; 26:795–800.
32. Brünger AT, Adams PD, Clore GM, DeLano WL, Gros P, Grosse-Kunstleve RW, Jiang JS, Kuszewski J, Nilges M, Pannu NS, Read RJ, Rice LM, Simonson T, Warren GL. *Acta Crystallogr D: Biol Crystallogr.* 1998; 54:905–921. [PubMed: 9757107]
33. Emsley P, Cowtan K. *Acta Crystallogr D: Biol Crystallogr.* 2004; 60:2126–2132. [PubMed: 15572765]
34. Lakowicz, JR. *Principles of fluorescence spectroscopy.* 2. Kluwer Academic/Plenum; New York: 1999. p. 54
35. Koellner G, Kryger G, Millard CB, Silman I, Sussman JL, Steiner T. *J Mol Biol.* 2000; 296:713–735. [PubMed: 10669619]
36. Felder CE, Harel M, Silman I, Sussman JL. *Acta Crystallogr D Biol Crystallogr.* 2002; 58:1765–1771. [PubMed: 12351819]
37. Harel M, Hyatt JL, Brumshtein B, Morton CL, Yoon KJ, Wadkins RM, Silman I, Sussman JL, Potter PM. *Mol Pharmacol.* 2005; 67:1874–1881. [PubMed: 15772291]



38. Greenblatt HM, Guillou C, Guénard D, Argaman A, Botti S, Badet B, Thal C, Silman I, Sussman JL. *J Am Chem Soc.* 2004; 126:15405–15411. [PubMed: 15563167]
39. Haviv H, Wong DM, Greenblatt HM, Carlier PR, Pang YP, Silman I, Sussman JL. *J Am Chem Soc.* 2005; 127:11029–11036. [PubMed: 16076210]
40. Dvir H, Wong DM, Harel M, Barril X, Orozco M, Luque FJ, Muñoz-Torrero D, Camps P, Rosenberry TL, Silman I, Sussman JL. *Biochemistry.* 2002; 41:2970–2981. [PubMed: 11863435]
41. Friedhoff P, Schneider A, Mandelkow EM, Mandelkow E. *Biochemistry.* 1998; 37:10223–10230. [PubMed: 9665729]
42. Kung CE, Reed JK. *Biochemistry.* 1986; 25:6114–6121.
43. Loutfy RO, Arnold BA. *J Phys Chem.* 1982; 86:4205–4211.
44. Wong DM, Greenblatt HM, Dvir H, Carlier PR, Han YF, Pang YP, Silman I, Sussman JL. *J Am Chem Soc.* 2003; 125:363–373. [PubMed: 12517147]
45. Rydberg EH, Brumshtein B, Greenblatt HM, Wong DM, Shaya D, Williams LD, Carlier PR, Pang YP, Silman I, Sussman JL. *J Med Chem.* 2006; 49:5491–5500. [PubMed: 16942022]

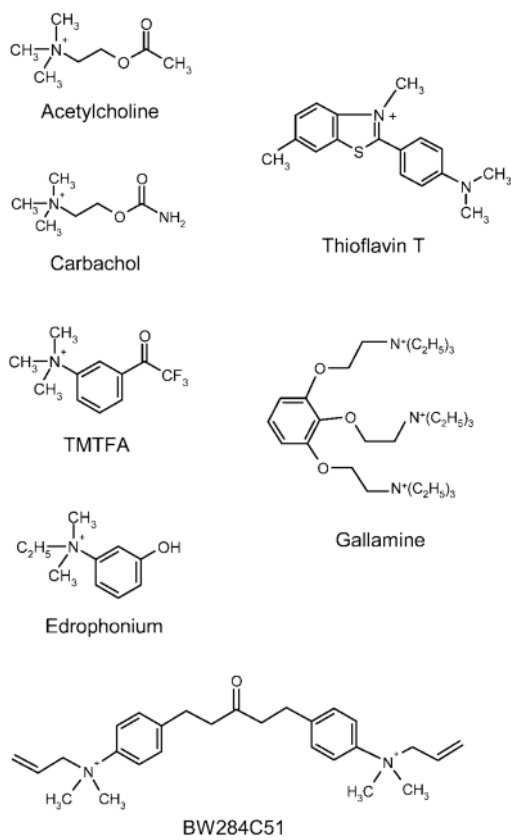


**Figure 1.**  
Chemical structures of AChE ligands discussed in the text.

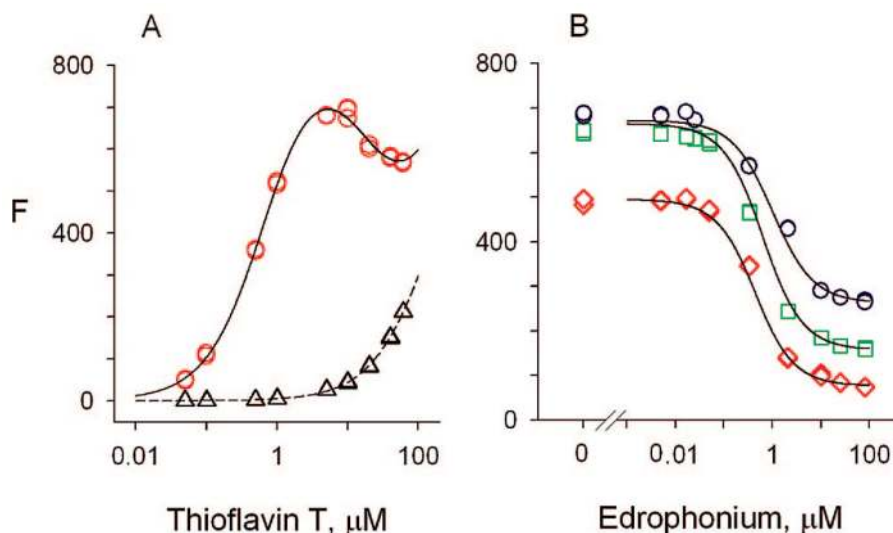


**Figure 2.**

(A) Fluorescence titrations of *TcAChE* with ThT. Fluorescence values ( $F$ ) were measured as outlined in the Methods at the indicated total concentrations of ThT. The fluorescence intensity coefficient for the free ligand ( $f_L$ ) was obtained from the plot in the absence of AChE ( $\Delta$ ). The fluorescence  $F$  in the presence of a fixed concentration of *TcAChE* (170 nM) ( $\circ$ ) was then analyzed as outlined in the Experimental Procedures. Values of  $K_{Lp} = 0.6 \pm 0.3 \mu\text{M}$  and  $f_{ELp}/f_L = 1200 \pm 300$  were obtained. (B) EDR binding decreases the fluorescence of *TcAChE*-bound ThT. The fluorescence values ( $F$ ) of mixtures of *TcAChE* (168 nM), ThT ( $\circ$ , 10  $\mu\text{M}$ ;  $\square$ , 3  $\mu\text{M}$ ;  $\diamond$ , 1  $\mu\text{M}$ ), and the indicated concentration of EDR were determined.  $F$  values from all three data sets were fitted with the SCoP program simultaneously as outlined in the Experimental Procedures. The fitting gave  $K_{Lp} = 0.7 \pm 0.2 \mu\text{M}$  for ThT;  $K_I = 190 \pm 10 \text{ nM}$  for EDR;  $K_{LpI}/K_I = 4 \pm 1$ ; and  $f_{ELpI}/f_{ELpI} = 3.4 \pm 0.6$ .

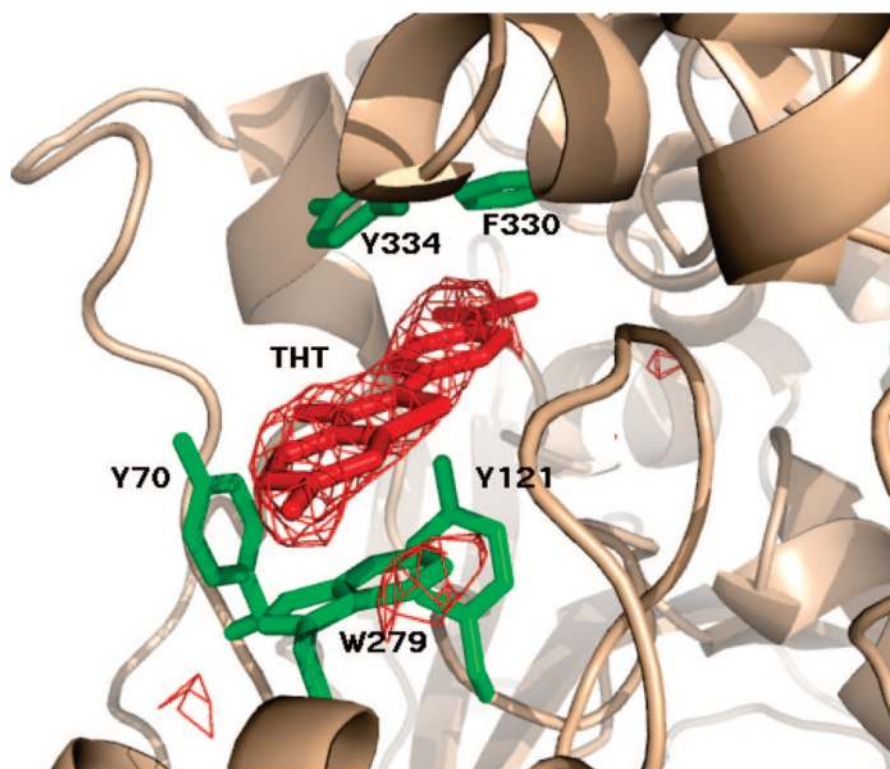


**Figure 3.** ThT (red) and its omit electron density map (Fo-Fc drawn at  $3\sigma$ ) in the ThT/TcAChE complex makes short contacts ( $<3.7\text{\AA}$ ) with five aromatic residues (green) in the active-site gorge.

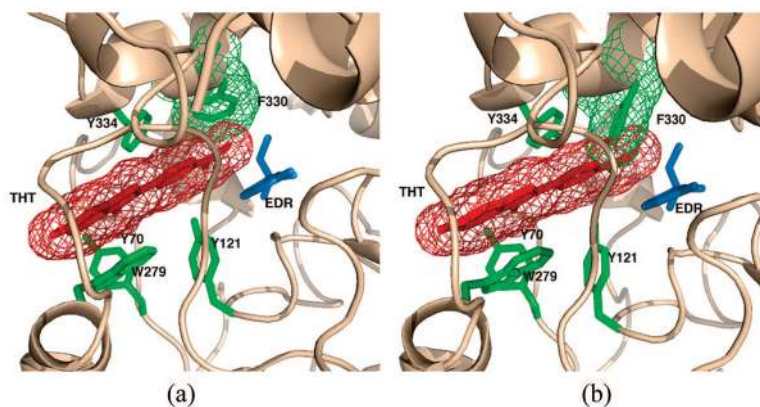
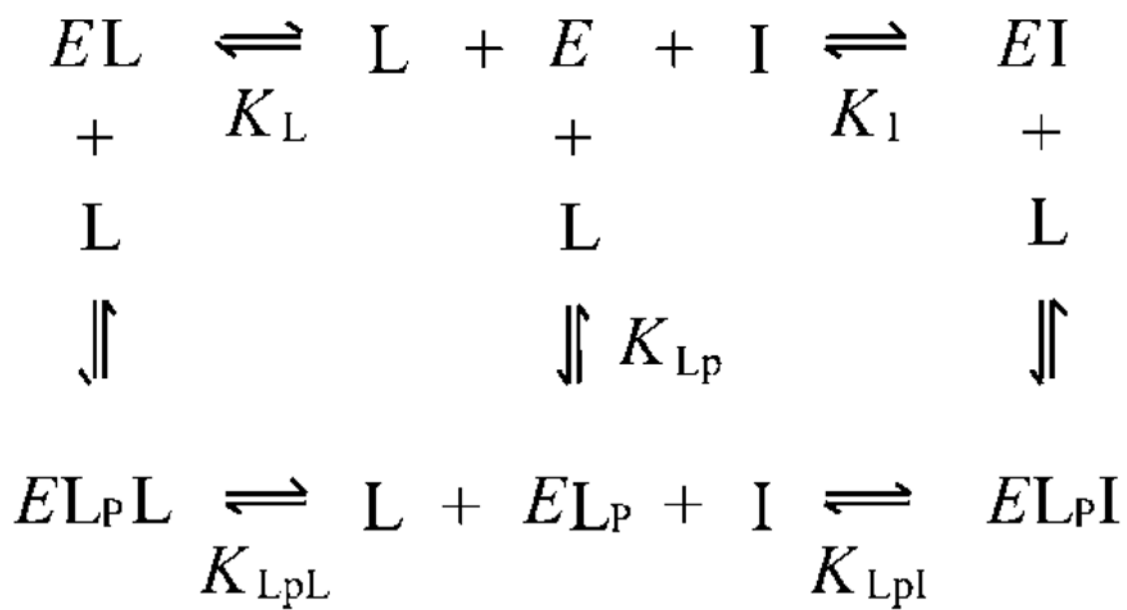


**Figure 4.** Models of the putative EDR/ThT/TcAChE ternary complex. (a) Crystal structure of the ThT/TcAChE complex, with a model of EDR, taken from the crystal structure of the EDR/TcAChE structure (PDB code 2ACK) superimposed. A  $\pi$ - $\pi$  stacking system, spanning the P- and A-sites, is formed by ThT (red mesh), EDR (blue stick model), Trp279, Tyr334 (both green stick models) and Phe330 (green mesh). (b) Crystal structure of the EDR/TcAChE complex (PDB code 2ACK), with a model of ThT taken from the ThT/TcAChE crystal structure superimposed. It can be seen that in the conformation that Phe330 (green mesh) adopts in the EDR complex, it clashes severely with the dimethylaminophenyl moiety of the ThT molecule.





Scheme 1.

**Table 1**

## Data Collection and Refinement Statistics

resolution	2.8 Å
wavelength	1.5418 Å
space group	$P3_221$
unit cell	$a = b = 139.44$ Å, $c = 71.42$ Å
data completeness	99.1%
$R_{\text{sym}}$	14.5%
$I/\sigma$	24.5 (8.4) <sup>a</sup>
$R$ -factor	19.6%
$R$ -free	25.1%

<sup>a</sup>Number in parentheses is value for highest resolution shell 2.8–2.9 Å.